Monoclonal antibody targeting the β-barrel assembly machine of *Escherichia coli* is bactericidal

Kelly M. Storek[a], Marcy R. Auerbach[a], Handuo Shi[a], Natalie K. Garcia[b], Dawei Sun[c], Nicholas N. Nickerson[a], Rajesh Vij[d], Zhonghua Lin[d], Nancy Chiang[d], Kellen Schneider[d], Aaron T. Wecksler[b], Elizabeth Skippington[e], Gerald Nakamura[d], Dhaya Seshasayee[d], James T. Koerber[d], Jian Payandeh[c], Peter A. Smith[a], and Steven T. Rutherford[a,1]

[a]Department of Infectious Diseases, Genentech Inc., South San Francisco, CA 94080; [b]Department of Protein Analytical Chemistry, Genentech Inc., South San Francisco, CA 94080; [c]Department of Structural Biology, Genentech Inc., South San Francisco, CA 94080; [d]Department of Antibody Engineering, Genentech Inc., South San Francisco, CA 94080; and [e]Department of Bioinformatics and Computational Biology, Genentech Inc., South San Francisco, CA 94080

The folding and insertion of integral β-barrel membrane proteins into the outer membrane of Gram-negative bacteria is required for viability and bacterial pathogenesis. Unfortunately, the lack of selective and potent modulators to dissect β-barrel folding in vivo has hampered our understanding of this fundamental biological process. Here, we characterize a monoclonal antibody that selectively inhibits an essential component of the *Escherichia coli* β-barrel assembly machine, BamA. In the absence of complement or other immune factors, the unmodified antibody MAB1 demonstrates bactericidal activity against an *E. coli* strain with truncated LPS. Direct binding of MAB1 to an extracellular BamA epitope inhibits its β-barrel folding activity, induces periplasmic stress, disrupts outer membrane integrity, and kills bacteria. Notably, resistance to MAB1-mediated killing reveals a link between outer membrane fluidity and protein folding by BamA in vivo, underscoring the utility of this antibody for studying β-barrel membrane protein folding within a living cell. Identification of this BamA antagonist highlights the potential for new mechanisms of antibiotics to inhibit Gram-negative bacterial growth by targeting extracellular epitopes.

Gram-negative bacteria | β-barrel protein | membrane protein folding | LPS | BamA

The outer membrane (OM) of Gram-negative bacteria is an essential and asymmetric structure that functions as a permeability barrier to cytotoxic molecules, including antibiotics (1). The OM is comprised of glycerophospholipids in the inner leaflet and lipopolysaccharide (LPS) in the outer leaflet (2). The large repetitive glycan polymer of LPS can prevent binding of extracellular factors such as antibodies (3), while the dense hydrocarbon chain packing and tight lateral interactions of LPS establish a formidable permeability barrier (1). Integral outer membrane proteins (OMPs) embedded in this distinctive asymmetric bilayer are crucial for multiple cellular functions, including construction of the OM itself, nutrient acquisition, and antibiotic efflux (4, 5). To assume their proper β-barrel folds, efficient folding and insertion of OMPs requires a dedicated protein complex (4, 6, 7). The recently discovered β-barrel assembly machine (BAM) performs this essential OMP folding process (8). Because depletion of the BAM complex is detrimental to bacterial viability and genetic mutations interfering with the BAM complex cause growth defects, BAM is an attractive antibacterial target (9–13). However, there are no examples of BAM antagonists with therapeutic potential, and no selective and potent pharmacological modulators of BAM function have been reported.

The central component of the BAM complex, BamA, is essential and conserved across Gram-negative bacteria (14). In *Escherichia coli*, the N-terminal periplasmic polypeptide transport-associated (POTRA) domains of BamA function in concert with four OM lipoproteins, BamB, BamC, BamD, and BamE, to receive nascent OMP substrates (13, 15–17). The C-terminal domain of BamA is a 16-stranded β-barrel OMP that exposes eight loops on the cell surface (16, 18–20). Proposed roles for the β-barrel structure of BamA include directed folding of OMPs through β-strand complementation, local distortion of the OM, and lowering the kinetic

barrier imposed by glycerophospholipids on OMP folding (6, 7, 20, 21). Although BamA receives substrates from the periplasmic side, mutations in the extracellular loops of BamA can interfere with activity (22, 23). The discovery of a BamA antagonist that targets these extracellular surface loops may overcome three major hurdles to Gram-negative antibiotic discovery: OM penetrance, drug inactivation, and efflux (24).

We recently developed an approach to enrich for the discovery of rare monoclonal antibodies (mAbs) targeting *E. coli* BamA. Here, we describe the functional characterization of a mAb that antagonizes BamA (MAB1) by binding to an extracellular epitope. MAB1 is bactericidal and establishes BamA as a potential antibacterial target on the surface of Gram-negative bacteria. MAB1 is a rare example of a selective and potent inhibitor of a membrane protein foldase, and we use this tool to probe β-barrel OMP folding in vivo. We observe genetic and conditional requirements for MAB1 inhibitory activity and establish an unexpected link between OMP folding by BamA and membrane fluidity in living cells.

Significance

The outer membrane of Gram-negative bacteria presents a formidable barrier to the discovery of new antibiotics needed to combat infections by multidrug-resistant bacteria. Targeting essential proteins or processes directly exposed to the environment could bypass this obstacle. Here, we describe a monoclonal antibody that selectively and potently antagonizes BamA, which folds and inserts integral outer membrane β-barrel proteins, by binding to a surface-exposed BamA epitope and, as a result, inhibits bacterial cell growth. Mechanisms of resistance to the antibody reveal that membrane fluidity affects BamA activity. This antibody validates the potential therapeutic strategy of targeting essential, exposed functions and provides a powerful tool for dissecting the fundamental process of folding integral membrane β-barrel proteins in vivo.

MAB1 Is a Bactericidal Antibody

Antibodies represent an ideal molecular scaffold to test whether BamA function can be inhibited extracellularly due to their high target affinity and selectivity. Because LPS is known to prevent mAb binding to OMPs (3), we used an *E. coli* strain ($\Delta waaD$) displaying the minimal LPS structure required for viability, allowing for maximal access to epitopes on the bacterial cell surface (3, 25, 26). Using an approach to enrich for BamA-specific mAbs, we screened >1,600 α-BamA IgG mAbs and identified 7 that completely inhibited *E. coli* $\Delta waaD$ growth. We purified five of these mAbs with reproducible growth inhibitory activity and found that all of these mAbs competed with each other for binding to BamA in vitro. Here, we focused our characterization on a representative inhibitory α-BamA mAb, MAB1.

Addition of purified MAB1 to a culture of *E. coli* $\Delta waaD$ led to a time-dependent decrease in the number of viable bacterial cells, demonstrating that it is bactericidal against this strain (Fig. 1A). At 4 h after addition of MAB1, the number of colony-forming units (CFUs) decreased by ~50-fold, while CFUs in the presence of a noninhibitory α-BamA mAb, MAB2, increased by ~50-fold (Fig. 1A). MAB2 is one of thousands of α-BamA mAbs that bound to purified BamA and to whole bacterial cells but did not inhibit growth (Fig. 1A and *SI Appendix*, Fig. S1). Unlike MAB1, however, MAB2 bound both the wild-type and $\Delta waaD$ *E. coli* (*SI Appendix*, Fig. S1), indicating it binds a more accessible epitope on BamA. While the genetic essentiality of *bamA* has been established (10), MAB1 is a potent pharmacological modulator of BamA and is a rare example of a naked bactericidal antibody (27).

Consistent with the high affinity of mAbs for their molecular targets, growth inhibition by MAB1 was concentration-dependent and required ~2 nM mAb to completely prevent growth (Fig. 1B). A monovalent antigen-binding fragment (Fab) also showed concentration-dependent growth inhibition activity (Fig. 1B). This eliminates the possibility that molecular crowding of BamA or mAb-mediated cell aggregation is responsible for the bactericidal activity of MAB1. Rather, the activity of the MAB1 Fab demonstrates that targeting a discrete extracellular epitope on BamA is sufficient for bactericidal activity.

To establish the molecular selectivity and cellular target of MAB1, we exploited the fact that this mAb binds *E. coli* BamA, but not purified BamA protein from the related *Enterobacteriaceae* species (*SI Appendix*, Fig. S2A). We created three $\Delta waaD$ strains with BamA chimeras by replacing the *E. coli bamA* β-barrel coding sequence with that from *Klebsiella pneumoniae*, *Enterobacter aerogenes*, or *Enterobacter cloacae*, while the N-terminal POTRA domains remained wild-type *E. coli*. Employing these BamA chimeric strains, we measured whole bacterial cell binding in vivo using a fluorescent-activated cell-sorting (FACS) assay and found that MAB1 did not bind (Fig. 1C and *SI Appendix*, Fig. S2B). Importantly, MAB1 did not inhibit the growth of these BamA chimeric strains (Fig. 1D), establishing that MAB1 is highly selective for the

E. coli BamA β-barrel and functions by binding to a critical epitope accessible on the surface of *E. coli* $\Delta waaD$.

MAB1 Is a BamA Antagonist

Having demonstrated that MAB1 binds *E. coli* BamA with high molecular selectively, we set out to investigate its mechanism of bacterial cell killing. To assess the ability of MAB1 to inhibit the essential β-barrel OMP folding activity of BamA, we monitored select OMP levels by Western blot after treatment with MAB1 or the control MAB2. Levels of three OMPs, LptD, OmpA, and OmpC, were 3- to 11-fold lower in the presence of MAB1 while MAB2 had no effect (Fig. 2A). The levels of a cytoplasmic protein (GroEL), an inner membrane protein (MsbA), and an OM lipoprotein that does not require BamA for folding and insertion (Lpp) were all unchanged in the presence of MAB1 (Fig. 2A). We also observed decreases in OMPs by SDS/PAGE analysis of OM preparations after MAB1 treatment, but not global changes in whole-cell lysates (*SI Appendix*, Fig. S3A). We conclude that MAB1 directly antagonizes OMP folding by BamA, establishing it as a rare membrane protein foldase inhibitor and a pharmacological tool to probe the BAM complex in vivo.

Under extreme growth conditions, the presence of unfolded OMPs in the periplasm activates stress response pathways that facilitate folding or removal of these OMPs (28). Because the binding of MAB1 directly antagonizes BamA (Fig. 2A), we measured activation of a reporter for the canonical σ^E periplasmic stress response to determine if unfolded OMPs accumulate in the periplasm (29). Addition of MAB1 resulted in time-dependent σ^E activation relative to the control MAB2 (Fig. 2B). BamA antagonism by MAB1 in vivo therefore activates pathways intended to resolve defects in OMP assembly.

Activity of the BAM complex is critical to maintaining the OM barrier function (11, 12, 30). To determine the effect of MAB1 on OM integrity, we measured permeability of ethidium bromide (EtBr), which cannot penetrate an intact OM. MAB1, but not the control MAB2, caused a dose-dependent increase in EtBr uptake (Fig. 2C). As further evidence, an antibiotic impeded by an intact OM, rifampicin (1), was potentiated eightfold by a subinhibitory concentration of MAB1 while mAb treatment had little or no effect on the activities of gentamicin or colistin, antibiotics not blocked by the OM (*SI Appendix*, Table S1). Finally, we used fluorescence microscopy to visualize *E. coli* $\Delta waaD$ strains expressing cytoplasmic GFP and periplasmic mCherry. During exposure to MAB1, we observed a rapid loss of periplasmic mCherry (<15 min) that preceded loss of cytoplasmic GFP (>90 min) (Fig. 2D and *SI Appendix*, Fig. S3B). This sequence of OM permeabilization preceding cytoplasmic membrane disruption is distinct from the simultaneous loss of OM and inner membrane integrity after treatment with a β-lactam antibiotic that inhibits peptidoglycan synthesis (31). We have therefore established that MAB1 directly antagonizes BamA function, which activates periplasmic stress responses and compromises OM integrity.
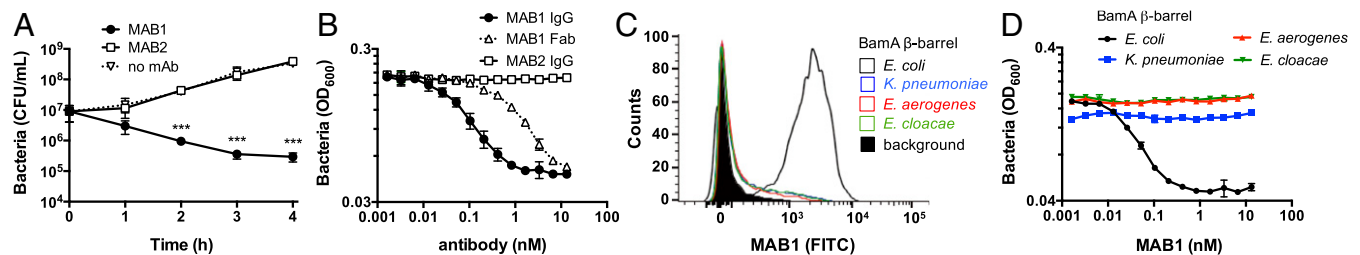

Fig. 1. α-BamA mAb MAB1 kills *E. coli* $\Delta waaD$. (A) CFUs were quantified at indicated times after the addition of 10 nM MAB1, MAB2, or no antibody to the *E. coli* $\Delta waaD$ strain. (B) Growth inhibition was measured by *E. coli* $\Delta waaD$ density (OD$_{600}$) in the presence of MAB1 IgG, MAB2, or MAB1 Fab after 4 h. (C) Representative FACS traces of MAB1 surface-binding to *E. coli* $\Delta waaD$ strains producing chimeric BamA proteins. The shaded trace is a control with no primary mAb. Mean fluorescent intensities (MFIs) for biological triplicate experiments are plotted in *SI Appendix*, Fig. S2B. (D) MAB1 dose–response inhibition of *E. coli* $\Delta waaD$ strains producing chimeric BamA measured by OD$_{600}$ after 4 h of treatment. For all experiments, means and SDs of biological triplicates are plotted. Unpaired *t* tests were used to compare values to untreated controls or IC$_{50}$ values. IC$_{50}$ values are in *SI Appendix*, Table S3. ***P < 0.001.
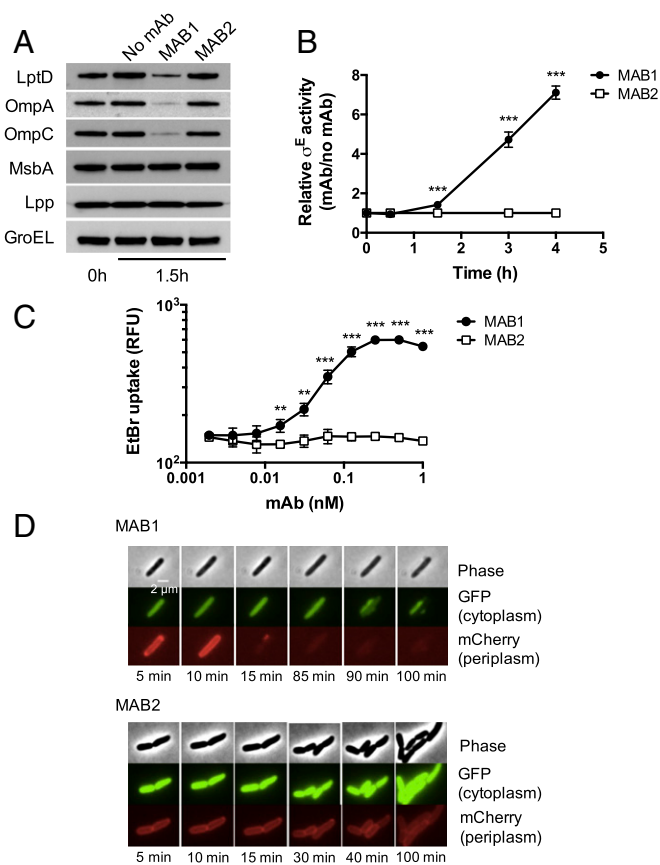
MICROBIOLOGY

Fig. 2. MAB1 inhibits BamA OMP folding activity. (A) Representative Western blots of OMPs and controls from *E. coli* ΔwaaD in the presence or absence of 10 nM MAB1 or MAB2 after 1.5 h of treatment. (B) Induction of σ^E periplasmic stress response (*rpoH* P3-*lacZ*) in *E. coli* ΔwaaD by 10 nM MAB1 or MAB2. Data are a ratio of mAb to no mAb at times after mAb addition. (C) Influx of EtBr (ex515 nm, em600 nm, normalized to OD_{600}) into *E. coli* ΔwaaD after MAB1 or MAB2 treatment. (D) Fluorescence time-lapse microscopy of *E. coli* ΔwaaD cells expressing GPF (cytoplasm) and mCherry (periplasm) pretreated with 13 nM MAB1 or MAB2 for 1.5 h and imaged for 3 h. A representative image is shown. Means and SDs of biological triplicates are plotted in *B* and *C*. Unpaired *t* tests were used to compare values at each time point or antibody concentration tested. **$P < 0.01$, ***$P < 0.001$.

MAB1 Binds to an Ion Pair on BamA Extracellular Loop 4

To identify the molecular determinants of its binding site, we exploited the *E. coli* species selectivity of MAB1 (Fig. 1*C*) and constructed *bamA* mutants that resulted in amino acid substitutions at positions unique to the extracellular loops of *E. coli* BamA (*SI Appendix*, Fig. S4). Of all of the BamA variants studied (*SI Appendix*, Fig. S5*A*), only substitutions E554Q and H555Y within extracellular loop 4 (L4) decreased MAB1 whole-cell binding (Fig. 3*A* and *SI Appendix*, Fig. S5*B*). BamA E554Q and H555Y provided resistance to bacterial growth inhibition by MAB1, and the combined E554Q/H555Y double substitution had a larger effect (Fig. 3 *A* and *B*). The E554Q/H555Y BamA also provided resistance to the other four inhibitory mAbs identified in our initial screen (*SI Appendix*, Fig. S5*C*), indicating that these active mAbs share similar binding determinants. Mutations at other L4 positions tested remained sensitive to MAB1 (Fig. 3*B*), suggesting that positions E554 and H555 represent an essential hotspot for MAB1 binding. Importantly, MAB2 bound *E. coli* ΔwaaD expressing all BamA L4 variants indistinguishably from wild-type BamA, indicating that none of these amino acid substitutions affected the level of accessible BamA on the cell surface (*SI Appendix*, Fig. S5*D*). We employed an orthogonal method, in vitro hydroxyl radical footprinting using purified proteins, to confirm that BamA L4 is

protected upon MAB1 binding (*SI Appendix*, Fig. S6). Consistent with MAB1 and MAB2 having distinct epitopes, MAB2 did not bind to BamA lacking extracellular loop 6 (L6), while MAB1 did, implicating L6 as a binding determinant for the inactive MAB2 (*SI Appendix*, Fig. S5 *A* and *D*). This finding potentially rationalizes the increased access of MAB2 to the wild-type *E. coli* strain (*SI Appendix*, Fig. S1) given the prominence of this BamA surface feature (18–20). Thus, MAB1 binding and bactericidal activity requires L4 positions that are distally located from the features of BAM typically considered to be important for function, including the lateral gate, the POTRA domains, the BamBCDE lipoproteins, and periplasmic chaperones (Fig. 3*C*).
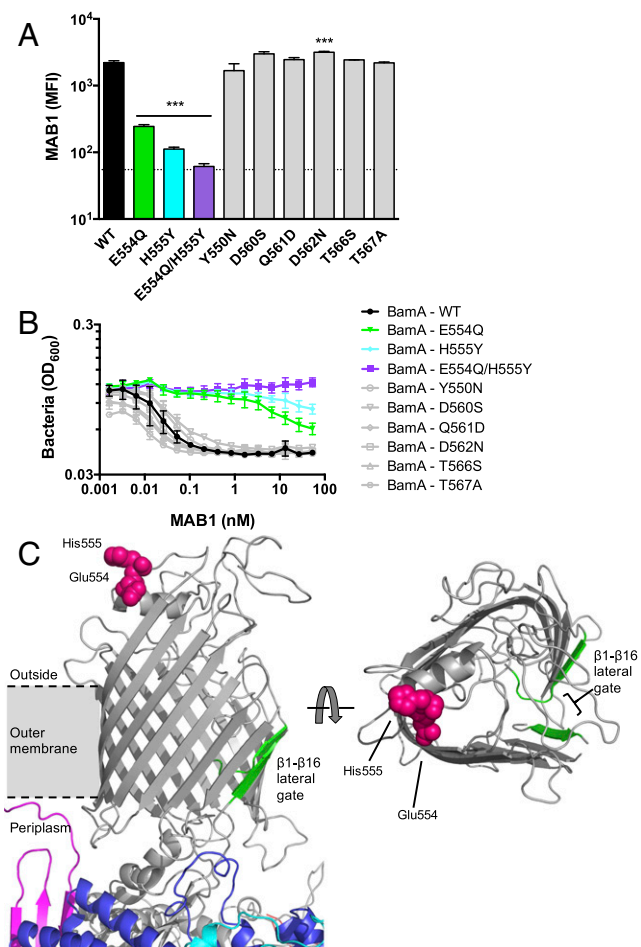

Fig. 3. MAB1 binds to BamA extracellular loop 4 (L4). *E. coli* ΔwaaD producing BamA with site-directed substitutions in L4 were quantified and compared for FACS whole cell binding by MAB1 (*A*) and growth inhibition by MAB1 by bacterial density (OD_{600}) (*B*). BamA variants with reduced MAB1 binding and sensitivity shown in color; substitutions with no or subtle effects on activity of MAB1 are gray. Means and SDs of biological triplicates are plotted. The dotted line is the background control with no mAb. IC_{50} values were calculated and compared with BamA – WT (0.018 ± 0.005 nM) by unpaired *t* test: E554Q (38.6 ± 7.2 nM, $P < 0.01$), H555Y (>50 nM, $P < 0.001$), E554Q/H555Y (>50 nM, $P < 0.001$), Y550N (0.030 ± 0.005 nM), D560S (0.038 ± 0.008 nM), Q561D (0.014 ± 0.002 nM), D562N (0.017 ± 0.003 nM), T566S (0.013 ± 0.005 nM), and T567A (0.011 ± 0.002 nM). (*C*) BAM rendered in PyMol from 5EKQ coordinates (16). BamA (gray), BamB (red), BamC (cyan), BamD (blue), and BamE (violet) are shown. Residues 554 and 555 are pink spheres. The β1-β16 lateral gate is indicated in green. The membrane space is approximated. *Left* and *Right* are rotated 90 °C relative to each other (BamBCDE are hidden in top view). Unpaired *t* tests were used to compare MFIs to WT or IC_{50} values for each strain tested. ***$P < 0.001$.

MAB1 Activity Depends on OM Fluidity

As a potent and selective antagonist of OMP folding, MAB1 represents a unique tool to identify additional cellular requirements for BamA function in vivo. We selected >50 spontaneous MAB1-resistant *E. coli* mutants, occurring at a frequency of $>1 \times 10^{-6}$, and found that all strains encoded wild-type *bamA*. Whole-genome sequencing of MAB1-resistant isolates revealed four distinct mutant *lpxM* alleles (*SI Appendix*, Fig. S7). LpxM transfers a myristate to penta-acylated Kdo_2-lipid IV_A resulting in hexa-acylated Kdo_2-lipid A during LPS biogenesis (32), which is expected to directly affect the structure of the OM bilayer (Fig. 4A). To confirm a role for *lpxM* in the inhibitory activity of MAB1, we deleted the entire *lpxM* coding region in the *E. coli* Δ*waaD* strain. This *E. coli* Δ*waaD*, Δ*lpxM* double mutant was resistant to MAB1 (Fig. 4B), and a plasmid expressing wild-type *lpxM* in this strain restored sensitivity (Fig. 4B). Notably, deletion of *lpxM* did not change OMP levels compared with the parental strain in the absence of MAB1, implying that LpxM itself does not profoundly alter OMP biogenesis, and, moreover, addition of MAB1 only decreased OMP levels ≤50% in this strain compared with a 3- to 11-fold decrease in the *E. coli* Δ*waaD* strain (*SI Appendix*, Figs. S3A and S8A). Importantly, MAB1 bound equally well to the *E. coli* Δ*waaD*, Δ*lpxM* double mutant and *E. coli* Δ*waaD* parental strain (Fig. 4C and *SI Appendix*, Fig. S8B). This result is in stark contrast to the L4 E554Q and H555Y substitutions where resistance was due to a lack of MAB1 binding (Fig. 3A). Thus, deletion of *lpxM* was sufficient to decouple the inhibitory activity of MAB1 from its BamA binding activity.
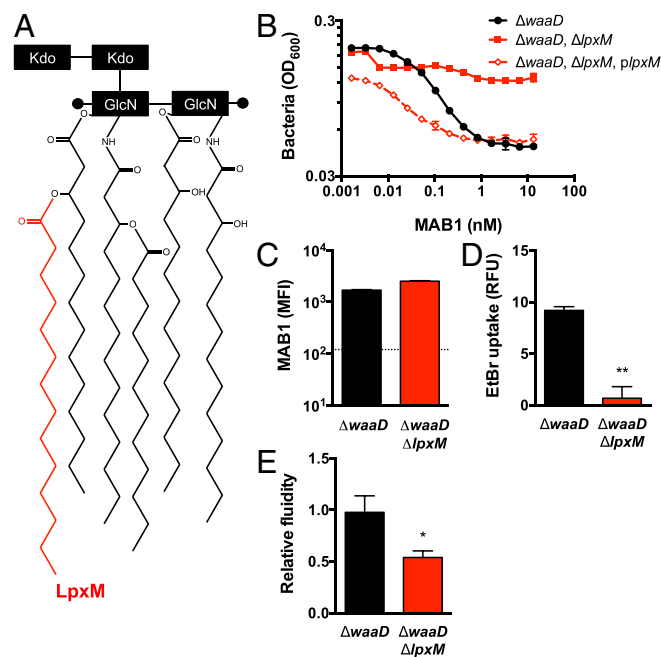
Alterations to LPS are known to affect the permeability and fluidity of the OM (33–35). Due to the functional role of LpxM in altering LPS structure (Fig. 4A), we investigated the impact of deleting *lpxM* on OM properties. Deletion of *waaD*, which was required for MAB1 binding and activity, increases the permeability of the OM, making *E. coli* Δ*waaD* strains sensitive to antibiotics and detergents normally blocked by this barrier (25, 36). We found that deleting *lpxM* from the permeable *E. coli* Δ*waaD* strain decreased the uptake of the hydrophobic dye EtBr (Fig. 4D and *SI Appendix*, Fig. S8C), indicating an improved OM barrier function of this double mutant compared with the *E. coli* Δ*waaD* parental strain. Employing a fluorescent probe that reports on relative membrane fluidity (37), we observed that the Δ*waaD*, Δ*lpxM* double mutant exhibited decreased membrane fluidity relative to the *E. coli* Δ*waaD* parental strain (Fig. 4E). Thus, the altered LPS in the absence of LpxM imparted resistance to the α-BamA mAb MAB1, and this resistance was linked, perhaps paradoxically, to a decrease in membrane fluidity.

LPS core oligosaccharide, which is absent in the *E. coli* Δ*waaD* strain, reportedly increases the rigidity of the OM (38). To assess the contribution of the LPS inner core oligosaccharide on MAB1 activity, we examined an *E. coli* Δ*waaG* strain, which produces LPS with three inner core heptose sugars (39). The presence of these sugars in the *E. coli* Δ*waaG* strain indeed increased membrane rigidity compared with the *E. coli* Δ*waaD* strain (Fig. 5 A and B). Although MAB1 bound similarly to the *E. coli* Δ*waaD* and Δ*waaG* strains (Fig. 5C), *E. coli* Δ*waaG* was resistant to the MAB1 growth inhibitory activity (Fig. 5D). Therefore, the ability of MAB1 to antagonize BamA function is dependent on the structure of LPS and appears to correlate with membrane fluidity.

Based on the link we observed between LPS structure and MAB1 activity (Figs. 4 and 5 A–D), we hypothesized that altering OM, and specifically fluidity, by other mechanisms might also affect MAB1 activity. Ionic strength and temperature are two parameters known to influence membrane fluidity (40). The fluidity of *E. coli* Δ*waaD* membranes decreased as the concentration of NaCl in the media increased (Fig. 5 E and F), consistent with salt-mediated stabilization of membranes. Remarkably, increasing NaCl reduced MAB1 activity (Fig. 5G), whereas MAB1 binding was unaffected even at a high NaCl (171 mM) concentration (Fig. 5H). We also examined the effect of temperature. Compared with 37 °C (Figs. 1–4), we found that at 30 °C, a condition under which membrane fluidity is decreased (37, 40) (Fig. 5 I and J), the *E. coli* Δ*waaD* strain became resistant to inhibition by MAB1 (Fig. 5L). Conversely, at 42 °C, a condition under which membrane fluidity is known to increase (40) (Fig. 5I), the *E. coli* Δ*waaD* strain was sensitized to MAB1 activity (Fig. 5L). Critically, the extent of MAB1 binding to whole cells was similar at each growth temperature (Fig. 5K). Moreover, the resistance imparted by Δ*lpxM* to the *E. coli* Δ*waaD* strain could be ablated when grown at 42 °C (Fig. 5L, open symbols), suggesting that the increased rigidity of the OM imparted by Δ*lpxM* was overcome by the effects of the high temperature on the OM. Overall, the physiological requirements for MAB1 activity revealed a link between BamA OMP folding activity and membrane fluidity in vivo.

Fig. 4. An *E. coli* Δ*waaD*, Δ*lpxM* mutant is resistant to MAB1. (A) Cartoon of LPS Kdo_2-lipid A with the acyl chain added by LpxM in red. (B) MAB1 growth inhibition of *E. coli* Δ*waaD*; *E. coli* Δ*waaD*, Δ*lpxM*; and *E. coli* Δ*waaD*, Δ*lpxM*, p*lpxM* complemented strains by cell density (OD_{600}). IC_{50} values were calculated and compared with Δ*waaD* (0.068 ± 0.0029 nM) by unpaired *t* tests: Δ*waaD*, Δ*lpxM* (>13.3 nM, *P* < 0.001), and Δ*waaD*, Δ*lpxM*, p*lpxM* (0.017 ± 0.0013 nM, *P* < 0.001). (C) FACS whole-cell binding by MFI of MAB1 to the *E. coli* Δ*waaD* and Δ*waaD*, Δ*lpxM* strains. The dotted line is the background control with no mAb. (D) EtBr uptake into *E. coli* Δ*waaD* and Δ*waaD*, Δ*lpxM* strains measured in the absence of mAb. (E) Membrane fluidity of *E. coli* Δ*waaD* and Δ*waaD*, Δ*lpxM* strains measured using a fluorescent lipophilic probe, pyrenedecanoic acid (PDA), in the absence of mAb. The ratio of emission at 470 nm to emission at 405 nm normalized to the *E. coli* Δ*waaD* strain is shown. For all experiments, means and SDs of biological triplicates are plotted. Unpaired *t* tests were used to compare values to Δ*waaD* or IC_{50} values for each strain tested. **P* < 0.05, ***P* < 0.01.

Discussion

There are multiple models for how the BAM complex may fold and insert β-barrel proteins into the Gram-negative bacterial OM (15, 16, 18, 23, 41–45). In one model, the β-strands of the BamA lateral gate (Fig. 3C) are hypothesized to template the folding of nascent OMPs through β-strand complementation. In a second model, structural features of BamA are proposed to distort the OM bilayer to facilitate OMP insertion. Finally, BamA is proposed to lower the kinetic barrier to OMP folding imposed by glycerophospholipids, thereby preferentially directing OMPs to fold into the OM. While distinct in their molecular details, these folding models all share major roles for the BamA lateral gate and the BAM complex-periplasmic lipid interface.
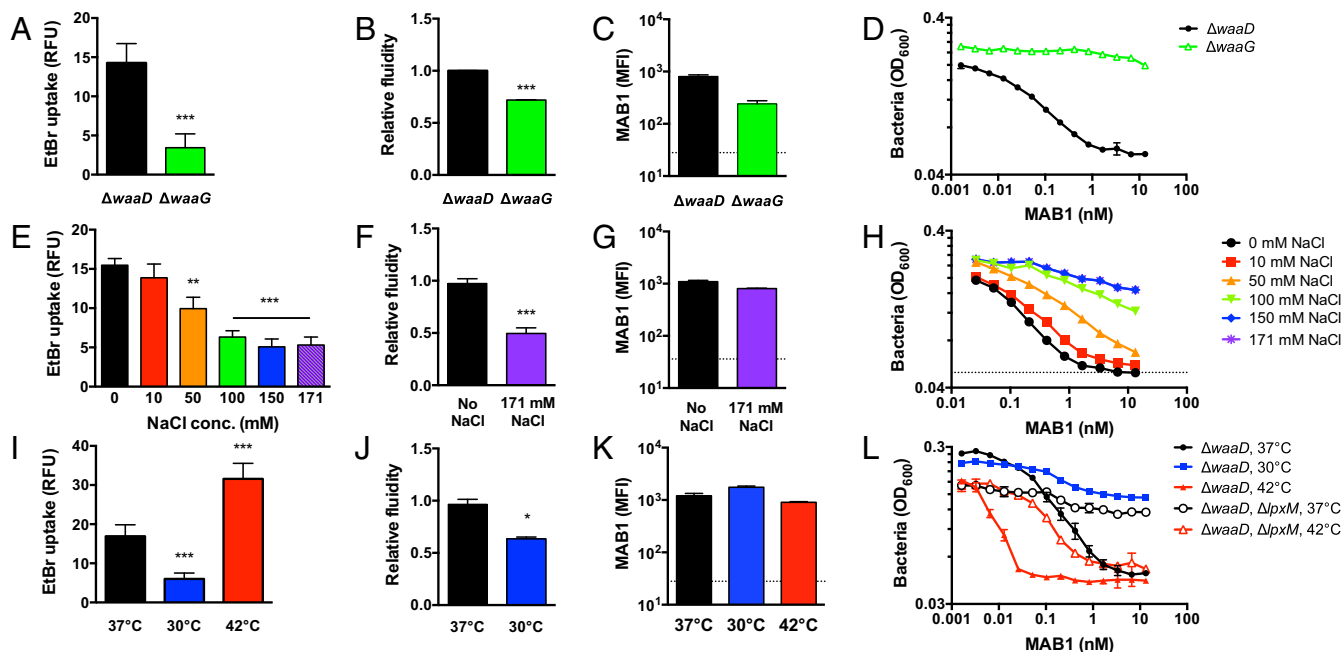
Fig. 5. LPS structure, NaCl concentration, and growth temperature change membrane fluidity and sensitivity to MAB1. (*A*, *E*, and *I*) EtBr uptake in *E. coli* Δ*waaD* cells compared with *E. coli* Δ*waaG* (*A*), grown at increasing NaCl concentrations (*E*), and grown at 37 °C, 30 °C, and 42 °C (*I*). Membrane fluidity of *E. coli* Δ*waaD* strain (*B*, *F*, and *J*), MAB1 whole-cell binding by FACS (*C*, *G*, and *K*), and growth inhibition by MAB1 of *E. coli* Δ*waaD* were compared with indicated strains and growth temperatures (*D*, *H*, and *L*). Membrane fluidity data are normalized to *E. coli* Δ*waaD* strain grown at 37 °C. High temperatures caused unequal fluidity probe integration (*SI Appendix*, Fig. S9). The dotted line is the control with no antibody. For all experiments, means and SDs of biological triplicates are plotted. Unpaired *t* tests were used to compare values to Δ*waaD* or Δ*waaD* 37 °C. IC$_{50}$ values are in *SI Appendix*, Table S3. *$P < 0.05$, **$P < 0.01$, ***$P < 0.001$.

We can envision three potential mechanisms for mAb-mediated inhibition of BamA activity. First, bridging of neighboring BAM complexes by a divalent antibody should increase molecular crowding with negative consequences for protein folding (46). However, the activity we observed for a monovalent Fab of MAB1 (Fig. 1*B*) eliminates this as the inhibitory mechanism. Second, cross-linking of the BamA lateral gate is lethal (41). However, direct lateral gate "stapling" cannot readily explain MAB1 activity because the L4 binding site is >40 Å away from the lateral gate (Fig. 3*C*), and there are conditions under which MAB1 remains bound to BamA but does not inhibit growth (Figs. 4 and 5). Thus, an allosteric mechanism for MAB1 activity is most parsimonious with our data because the L4 epitope of MAB1 is far removed from features previously implicated in BamA function (i.e., the lateral gate and periplasmic interface; Fig. 3*C*) and substitutions of L4 residues critical for binding are not lethal (Fig. 3). We note that specific insertions and deletions in BamA L4 have been found to disrupt *E. coli* growth (22) and, thus, may cause analogous allosteric effects on BamA function. Given that BamA is homologous to Sam50, a central component of the sorting and assembly machinery located in mitochondria and chloroplasts (47), we imagine that allosteric antagonism may be possible for these β-barrel foldases as well.

The physical state of the membrane bilayer is expected to affect the efficiency of membrane protein insertion and folding. Elegant in vitro studies have demonstrated a correlation between OMP folding and temperature with increased folding efficiency at higher temperatures, implicating a role for membrane fluidity (4, 48). We initially assumed, therefore, that BamA would be most sensitive to MAB1 inhibition when membrane fluidity is low (e.g., high NaCl or low temperature) because under these conditions, BamA would have to overcome the barrier imposed by a rigid membrane to fold OMPs. Paradoxically, however, we observed that BamA is most susceptible to inhibition when the OM is highly fluid (Figs. 4 and 5). Although speculative, our interpretation of these unanticipated results is that BamA activity may be suboptimal when the OM is in an excessively fluid state. Indeed, the pattern of major OMPs in the OM of the

MAB1-sensitive Δ*waaD* strain is distinct from that of a wild-type strain (*SI Appendix*, Fig. S3*A*). Consistent with this speculative model, overproduction of the major periplasmic chaperone SurA can decrease stress in the *E. coli* Δ*waaD* strain (49), presumably by binding to the unfolded OMPs that accumulate due to suboptimal BAM activity in this strain. Multiple hypotheses may explain why BamA appears to be defective under low membrane fluidity conditions within the cell. For instance, the structure of BamA may be altered, BamA could undergo excessive or futile structural fluctuations, or BAM complex formation could be defective. Our results highlight the importance of considering the membrane environment in which BamA is embedded when performing and interpreting in vivo and in vitro experiments. In summary, the allosteric α-BamA mAb antagonist MAB1 has revealed a potential role for membrane fluidity and LPS structure on BamA function in vivo.

In addition to representing a unique tool for studying OMP folding in vivo, MAB1 sheds light on the search for much needed Gram-negative bacterial therapeutics. Antimicrobial antibody therapies explored to date have generally either required additional immune system components, neutralized extracellular toxins, or utilized complex antibody formats (50–53). In contrast, MAB1 functions as an unmodified antibody with intrinsic antibacterial activity. Notably, the only other reported example of an intrinsically bactericidal mAb targets *Borrelia*, a species possessing a unique cholesterol-containing glycolipid OM lacking LPS (27). This mAb appears to produce holes in the bacterial membranes, but the molecular mechanism is unclear. Although, disappointingly, MAB1 falls short as a potential therapeutic due to its activity requirements, including limited epitope access (Fig. 1 *A* and *B*), it should motivate the search for additional antibodies or antibody formats (54) that target BamA. Importantly, the activity of MAB1 validates the approach of targeting an essential extracellularly accessible cellular process, which removes the constraints imposed by OM penetration and efflux (1, 24). This study may therefore guide future efforts to identify critical extracellular epitopes on pathogenic Gram-negative bacteria and

represents a potential step toward discovering novel classes of antibiotics.

Materials and Methods

Detailed materials and methods are found in *SI Appendix*. Bacterial strains and primers are listed in *SI Appendix*, Table S2, and strain construction is described in *SI Appendix*. Unless indicated, bacteria were grown in Mueller Hinton II cation-adjusted broth with 0.002% Tween 80 and appropriate antibiotics to midlog phase. To raise mAbs, mice and rats were immunized with sublethal injections of *E. coli* bacteria and purified *E. coli* BamA protein. Hybridoma fusions were sorted and BamA-ELISA$^+$ supernatants were screened for activity. Growth inhibition assays were performed in sterile round-bottom 96-well plates incubated statically at 37 °C, and viability was monitored via CFUs. Whole-cell binding of mAbs was measured by FACS on a FACSAria using FACSDiva software (BD). Genomic DNA from spontaneous MAB1-resistant mutants was isolated and sequenced by Illumina HiSeq 2000. β-galactosidase (β-Glo Assay, Promega) and cell numbers (BacTiter-Glo Microbial Cell Viability Assay; Promega) were measured at indicated times to determine σ^E activity. Membrane fluidity was measured using the Abcam Membrane Fluidity Kit according to the manufacturer's instructions. HRF labeling was performed using the fast photochemical oxidation of proteins methodology. For microscopy experiments, cells were imaged at 100× on a Nikon Eclipse TE inverted fluorescence microscope (Nikon Instruments).

1. Nikaido H (2003) Molecular basis of bacterial outer membrane permeability revisited. *Microbiol Mol Biol Rev* 67:593–656.
2. Kamio Y, Nikaido H (1976) Outer membrane of *Salmonella typhimurium*: Accessibility of phospholipid head groups to phospholipase c and cyanogen bromide activated dextran in the external medium. *Biochemistry* 15:2561–2570.
3. Bentley AT, Klebba PE (1988) Effect of lipopolysaccharide structure on reactivity of antiporin monoclonal antibodies with the bacterial cell surface. *J Bacteriol* 170:1063–1068.
4. Kleinschmidt JH (2015) Folding of β-barrel membrane proteins in lipid bilayers—Unassisted and assisted folding and insertion. *Biochim Biophys Acta* 1848:1927–1943.
5. Silhavy TJ, Kahne D, Walker S (2010) The bacterial cell envelope. *Cold Spring Harb Perspect Biol* 2:a000414.
6. Gessmann D, et al. (2014) Outer membrane β-barrel protein folding is physically controlled by periplasmic lipid head groups and BamA. *Proc Natl Acad Sci USA* 111:5878–5883.
7. Noinaj N, Gumbart JC, Buchanan SK (2017) The β-barrel assembly machinery in motion. *Nat Rev Microbiol* 15:197–204.
8. Ricci DP, Silhavy TJ (2012) The Bam machine: A molecular cooper. *Biochim Biophys Acta* 1818:1067–1084.
9. Hagan CL, Wzorek JS, Kahne D (2015) Inhibition of the β-barrel assembly machine by a peptide that binds BamD. *Proc Natl Acad Sci USA* 112:2011–2016.
10. Wu T, et al. (2005) Identification of a multicomponent complex required for outer membrane biogenesis in *Escherichia coli*. *Cell* 121:235–245.
11. Malinverni JC, et al. (2006) YfiO stabilizes the YaeT complex and is essential for outer membrane protein assembly in *Escherichia coli*. *Mol Microbiol* 61:151–164.
12. Sklar JG, et al. (2007) Lipoprotein SmpA is a component of the YaeT complex that assembles outer membrane proteins in *Escherichia coli*. *Proc Natl Acad Sci USA* 104:6400–6405.
13. Knowles TJ, et al. (2011) Structure and function of BamE within the outer membrane and the β-barrel assembly machine. *EMBO Rep* 12:123–128.
14. Voulhoux R, Bos MP, Geurtsen J, Mols M, Tommassen J (2003) Role of a highly conserved bacterial protein in outer membrane protein assembly. *Science* 299:262–265.
15. Warner LR, Gatzeva-Topalova PZ, Doerner PA, Pardi A, Sousa MC (2017) Flexibility in the periplasmic domain of BamA is important for function. *Structure* 25:94–106.
16. Bakelar J, Buchanan SK, Noinaj N (2016) The structure of the β-barrel assembly machinery complex. *Science* 351:180–186.
17. Fleming PJ, et al. (2016) BamA POTRA domain interacts with a native lipid membrane surface. *Biophys J* 110:2698–2709.
18. Gu Y, et al. (2016) Structural basis of outer membrane protein insertion by the BAM complex. *Nature* 531:64–69.
19. Han L, et al. (2016) Structure of the BAM complex and its implications for biogenesis of outer-membrane proteins. *Nat Struct Mol Biol* 23:192–196.
20. Noinaj N, et al. (2013) Structural insight into the biogenesis of β-barrel membrane proteins. *Nature* 501:385–390.
21. Fleming KG (2015) A combined kinetic push and thermodynamic pull as driving forces for outer membrane protein sorting and folding in bacteria. *Philos Trans R Soc Lond B Biol Sci* 370:20150026.
22. Browning DF, et al. (2013) Mutational and topological analysis of the *Escherichia coli* BamA protein. *PLoS One* 8:e84512.
23. Rigel NW, Ricci DP, Silhavy TJ (2013) Conformation-specific labeling of BamA and suppressor analysis suggest a cyclic mechanism for β-barrel assembly in *Escherichia coli*. *Proc Natl Acad Sci USA* 110:5151–5156.
24. Lewis K (2013) Platforms for antibiotic discovery. *Nat Rev Drug Discov* 12:371–387.
25. Coleman WG, Jr, Leive L (1979) Two mutations which affect the barrier function of the *Escherichia coli* K-12 outer membrane. *J Bacteriol* 139:899–910.
26. Kneidinger B, et al. (2002) Biosynthesis pathway of ADP-L-glycero-beta-D-manno-heptose in *Escherichia coli*. *J Bacteriol* 184:363–369.
27. LaRocca TJ, et al. (2009) The bactericidal effect of a complement-independent antibody is osmolytic and specific to Borrelia. *Proc Natl Acad Sci USA* 106:10752–10757.
28. Raivio TL, Silhavy TJ (2001) Periplasmic stress and ECF sigma factors. *Annu Rev Microbiol* 55:591–624.
29. Walsh NP, Alba BM, Bose B, Gross CA, Sauer RT (2003) OMP peptide signals initiate the envelope-stress response by activating DegS protease via relief of inhibition mediated by its PDZ domain. *Cell* 113:61–71.
30. Onufryk C, Crouch ML, Fang FC, Gross CA (2005) Characterization of six lipoproteins in the sigmaE regulon. *J Bacteriol* 187:4552–4561.
31. Yao Z, Kahne D, Kishony R (2012) Distinct single-cell morphological dynamics under beta-lactam antibiotics. *Mol Cell* 48:705–712.
32. Clementz T, Zhou Z, Raetz CR (1997) Function of the *Escherichia coli* msbB gene, a multicopy suppressor of htrB knockouts, in the acylation of lipid A. Acylation by MsbB follows laurate incorporation by HtrB. *J Biol Chem* 272:10353–10360.
33. Rottem S, Leive L (1977) Effect of variations in lipopolysaccharide on the fluidity of the outer membrane of *Escherichia coli*. *J Biol Chem* 252:2077–2081.
34. Vaara M, Nurminen M (1999) Outer membrane permeability barrier in *Escherichia coli* mutants that are defective in the late acyltransferases of lipid A biosynthesis. *Antimicrob Agents Chemother* 43:1459–1462.
35. Wang Z, Wang J, Ren G, Li Y, Wang X (2015) Influence of core oligosaccharide of lipopolysaccharide to outer membrane behavior of *Escherichia coli*. *Mar Drugs* 13:3325–3339.
36. Liu A, et al. (2010) Antibiotic sensitivity profiles determined with an *Escherichia coli* gene knockout collection: Generating an antibiotic bar code. *Antimicrob Agents Chemother* 54:1393–1403.
37. Kumar GS, Jagannadham MV, Ray MK (2002) Low-temperature-induced changes in composition and fluidity of lipopolysaccharides in the antarctic psychrotrophic bacterium *Pseudomonas syringae*. *J Bacteriol* 184:6746–6749.
38. Brandenburg K, Seydel U (1990) Investigation into the fluidity of lipopolysaccharide and free lipid A membrane systems by Fourier-transform infrared spectroscopy and differential scanning calorimetry. *Eur J Biochem* 191:229–236.
39. Raetz CRH, Whitfield C (2002) Lipopolysaccharide endotoxins. *Annu Rev Biochem* 71:635–700.
40. Los DA, Murata N (2004) Membrane fluidity and its roles in the perception of environmental signals. *Biochim Biophys Acta* 1666:142–157.
41. Noinaj N, Kuszak AJ, Balusek C, Gumbart JC, Buchanan SK (2014) Lateral opening and exit pore formation are required for BamA function. *Structure* 22:1055–1062.
42. Rigel NW, Schwalm J, Ricci DP, Silhavy TJ (2012) BamE modulates the *Escherichia coli* β-barrel assembly machine component BamA. *J Bacteriol* 194:1002–1008.
43. Leonard-Rivera M, Misra R (2012) Conserved residues of the putative L6 loop of *Escherichia coli* BamA play a critical role in the assembly of β-barrel outer membrane proteins, including that of BamA itself. *J Bacteriol* 194:4662–4668.
44. Doerner PA, Sousa MC (2017) Extreme dynamics in the BamA β-barrel seam. *Biochemistry* 56:3142–3149.
45. Danoff EJ, Fleming KG (2015) Membrane defects accelerate outer membrane β-barrel protein folding. *Biochemistry* 54:97–99.
46. van den Berg B, Ellis RJ, Dobson CM (1999) Effects of macromolecular crowding on protein folding and aggregation. *EMBO J* 18:6927–6933.
47. Höhr AIC, Straub SP, Warscheid B, Becker T, Wiedemann N (2015) Assembly of β-barrel proteins in the mitochondrial outer membrane. *Biochim Biophys Acta* 1853:74–88.
48. Maurya SR, Chaturvedi D, Mahalakshmi R (2013) Modulating lipid dynamics and membrane fluidity to drive rapid folding of a transmembrane barrel. *Sci Rep* 3:1989.
49. Missiakas D, Betton JM, Raina S (1996) New components of protein folding in extracytoplasmic compartments of *Escherichia coli* SurA, FkpA and Skp/OmpH. *Mol Microbiol* 21:871–884.
50. Lehar SM, et al. (2015) Novel antibody-antibiotic conjugate eliminates intracellular S. aureus. *Nature* 527:323–328.
51. DiGiandomenico A, et al. (2014) A multifunctional bispecific antibody protects against *Pseudomonas aeruginosa*. *Sci Transl Med* 6:262ra155.
52. Kozel TR (2014) The road to toxin-targeted therapeutic antibodies. *MBio* 5:e01477.
53. Huang W, et al. (2016) Employing *Escherichia coli*-derived outer membrane vesicles as an antigen delivery platform elicits protective immunity against *Acinetobacter baumannii* infection. *Sci Rep* 6:37242.
54. Kadam RU, et al. (2017) Potent peptidic fusion inhibitors of influenza virus. *Science* 358:496–502.

MICROBIOLOGY